Highly Photostable Luminescent Poly(ϵ-caprolactone)siloxane Biohybrids Doped with Europium Complexes

M. Fernandes and V. de Zea Bermudez*

Departamento de Química and CQ-VR, Universidade de Trás-os Montes e Alto Douro, 5000-801 Vila Real, Portugal

R. A. Sá Ferreira and L. D. Carlos*

Departamento de Física and CICECO, Universidade de Aveiro, 3810-193 Aveiro, Portugal

A. Charas and J. Morgado

Instituto de Telecomunicações and Departamento de Eng Química, Instituto Superior Técnico, 1049-001 Lisboa, Portugal

M. M. Silva and M. J. Smith

Departamento de Química, Universidade do Minho, Gualtar, 4710-057 Braga, Portugal

Received November 28, 2006. Revised Manuscript Received May 22, 2007

In this paper, we propose for the first time that the combination of a sol−gel derived diurethane cross-linked siloxane-based biohybrid host including short poly(ϵ-caprolactone) segments (PCL(530)) and lanthanide aquocomplexes incorporating β-diketonate ligands yields an effective protecting cage that efficiently encapsulates the emitting centers and reduces luminescence quenching. The results obtained using the $Eu(tta)_3(H_2O)_2$ (where tta^- is 2-thenoyltrifluoracetonate) complex demonstrate that 1 (2) carbonyl oxygen atoms of the host matrix enter the Eu^{3+} coordination shell, thus replacing the labile water molecule-(s). The significant increase in the quantum efficiency *q* of the doped hybrid with respect to that of $Eu(tta)_3(H_2O)_2$ (44.2 versus 29.0%, respectively) reveals that complex anchoring to the PCL(530)-based host structure contributes to enhancement of the $^5D_0$ quantum efficiency. However, when a complex that contains only strong chelating ligands, such as $Eu(tta)_3$phen (where phen is 1,10-phenantroline), is incorporated into the same host medium, the effect is lost and the $^5D_0$ nonradiative paths in the doped hybrid are higher than those existing in the complex itself. Under UVA exposure, the emission intensity of PCL(530)/siloxane/$Eu(tta)_3(H_2O)_2$ decreased 10% in 11 h, whereas that of PCL(530)/siloxane/Eu-$(tta)_3$phen decreased 25% in the same period of time.

Introduction

Materials incorporating lanthanide ions (e.g., Nd^{3+}, Eu^{3+}, Er^{3+}, Tb^{3+}, Ce^{3+}) are of great interest for a wide range of optical applications, such as tunable lasers, luminescence displays, amplifiers for optical communication and optical storage based on photochemical hole burning.[1−4] In addition, Ce^{3+}-doped hosts may find application in the area of scintillation and tunable lasers in the UV and visible ranges.[5]

In recent years, the sol−gel process[6] has become one of the preferred synthetic routes for the development of organic/inorganic hybrids[7] with technological interest for the domain of optics. Because of its advantages, in particular, the mild reaction conditions, the processing versatility, the possibility of mixing the inorganic and organic precursor components at the nanometer scale,[8] and the ability of tailoring the final properties of the material through adequate choice of the organic and inorganic components,[9,10] this chemical method has been extensively employed for the creation of amorphous matrices with improved luminescence properties.

The synthesis and design of hybrid frameworks for optics, a challenging task for the materials research community, has

* Corresponding author. Tel: 351-259-350253; 351-234-370946 (L.D.C.). Fax: 351-259-350480 (V.d.Z.B.); 351-234-424965 (L.D.C.). E-mail: vbermude@utad.pt (V.d.Z.B.); lcarlos@fis.ua.pt (L.D.C.).

(1) McGehee, M. D.; Bergstedt, T.; Zhang, C.; Saab, A. P.; O'Regan, M. B.; Bazan, G. C.; Srdanov, V. I.; Heeger, A. J. *Adv. Mater.* **1999**, *11*, 1349.
(2) Adachi, C.; Baldo, M. A.; Forrest, S. R. *J. Appl. Phys.* **2000**, *87*, 8049.
(3) Kido, J.; Okamoto Y. *Chem. Rev.* **2002**, *102*, 2357.
(4) Bunzli, J.-C. G.; Piguet, C. *Chem. Soc. Rev.* **2005**, *34*, 1048.
(5) Sanchez, C.; Lebeau. B. *MRS Bull.* **2001**, 377.
(6) Brinker, C. J.; Scherer, G. W. *Sol−Gel Science: The Physics and Chemistry of Sol−Gel Processing*; Academic Press: San Diego, CA, 1990.
(7) Gomez-Romero, P.; Sanchez, C. *Functional Hybrid Materials*; Wiley-Interscience: New York, 2003.
(8) Hench, L. L; West, J. K. *Chem. Rev.* **1990**, *90*, 33.
(9) (a) Judeinstein, P.; Sanchez, C. *J. Mater. Chem.* **1996**, *6*, 511. (b) Sanchez, C.; Soler-Illia, G. J. A. A.; Ribot, F.; Lalot, T.; Mayer, C. R.; Cabuil, V. *Chem. Mater.* **2001**, *13*, 3061. (c) Soler-Illia, G. J. A. A.; Sanchez, C; Lebeau, B.; Patarin, J. *Chem. Rev.* **2002**, *102*, 4093. (d) Sanchez, C.; Julián, B.; Belleville, P.; Popall, M. *J. Mater. Chem.* **2005**, *15*, 3559. (e) Vallé, K.; Belleville, P.; Pereira, F.; Sanchez, C. *Nat. Mater.* **2006**, *5*, 107.
(10) Carlos, L. D.; Sá Ferreira, R. A.; de Zea Bermudez, V. In *Encyclopedia of Nanoscience and Nanotechnology*; Nalwa, H. S., Ed.; American Scientific Publishers: North Lewis Way, CA, 2003.

10.1021/cm062832n CCC: $37.00
Published on Web 07/17/2007

been essentially directed toward the reduction or virtual suppression of groups responsible for the luminescence quenching (e.g., silanol (Si−OH) groups and residual solvent). The following five strategies have been proposed:[5] (1) Fine control of the sol−gel processing conditions. This may be achieved by means of optimization of water content, use of reactive hydrophobic precursors and thermal curing. (2) Use of nonhydrolytic procedures, such as the modified sol−gel process, usually designated as solvolysis or carboxylic acid method.[11−13] (3) Combination of strategy 1 with the encapsulation of the emitting species through complexation or chelation. The complexes or chelates may be added directly to the matrix[14−18] or may be formed in situ.[19−21] In the latter case, appropriate ligands are grafted or anchored to the hybrid network itself prior to the addition of the lanthanide ions. (4) Encapsulation of the lanthanide ions within nanoparticles. This route involves the combination of microemulsion techniques with the sol−gel process.[22−24] (5) Simultaneous introduction of inorganic and organic chromophores, i.e., lanthanide ions and organic dyes, into the hybrid structure.

Embedding of luminescence species, such as dyes or lanthanide compounds (salts or complexes), into sol−gel-derived hybrid host structures (strategy 3) has attracted considerable interest in the past few years. Lanthanide complexes, in particular lanthanide β-diketonate chelates, exhibit intense emission lines upon UV light irradiation because of the effective intramolecular energy transfer from the coordinating ligands to the central lanthanide ions, which in turn undergo the corresponding radiative emitting process (the "antenna effect"[25]). However, in spite of the good luminescence features, the poor thermal stability and mechanical properties of lanthanide complexes have severely limited their practical application. A significant number of reports have demonstrated that a strategy that allows us to successfully overcome these disadvantages is the incorporation of these complexes into organic/inorganic host networks using low-temperature soft-chemistry routes, such as the sol−gel process.[26−34]

Scheme 1. Structures of the (A) PCL (530)/Siloxane Hybrid Host Matrix and (B) $Eu(tta)_3(H_2O)_2$, and (C) $Eu(tta)_3$phen Complexes

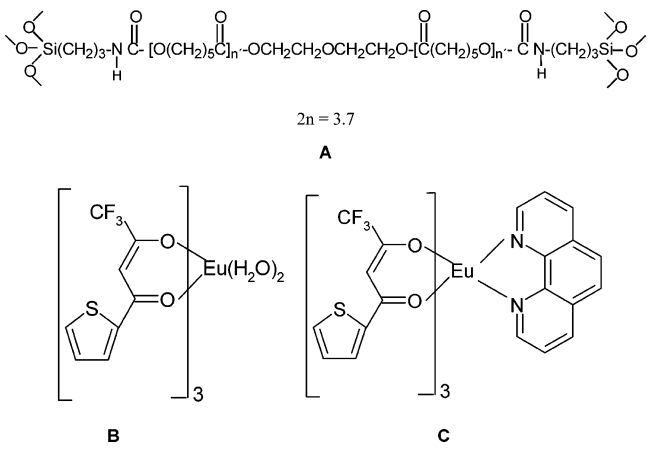

In this paper, we investigate the structure, morphology, thermal properties, and luminescence features of an innovative hybrid system composed of a sol−gel derived diurethane cross-linked siloxane-based host including short poly(ϵ-caprolactone) segments (abbreviated as PCL(530), where 530 represents the average molecular weight in g mol^{-1} [35] (Scheme 1A) and the $Eu(tta)_3(H_2O)_2$ and $Eu(tta)_3$phen complexes (B and C in Scheme 1, respectively).

The $Eu(tta)_3$phen complex has been extensively employed to produce luminescent organically modified silicate composite phosphors.[26,33,34]

In contrast, PCL is a linear, aliphatic thermoplastic, with a unique set of properties (biocompatibility, permeability, hydrophobicity, biodegradability, nontoxicity for living organisms, resorbtion after a certain period of implantation time), that has found widespread application in the field of medicine, as biodegradable suture, artificial skin, resorbable

(11) Pope, E. J. A.; Mackenzie, J. D. *J. Non-Cryst. Solids* **1986**, *87*, 185.
(12) Brankova, T.; Bekiari, V.; Lianos, P. *Chem. Mater.* **2003**, *15*, 1855.
(13) Stathatos, E.; Lianos, P.; Orel, B.; Surca Vuk, A.; Jese, R. *Langmuir* **2003**, *19*, 7587.
(14) Avnir, D.; Levy, D.; Reisfeld, R. *J. Phys. Chem.* **1984**, *88*, 5956.
(15) Maas, H.; Currao, A.; Calzaferri, G. *Angew. Chem., Int. Ed.* **2002**, *41*, 2495.
(16) Sanchez, C.; Lebeau, B.; Chaput, F.; Boilot, J.-P. *Adv. Mater*. **2003**, *15*, 1969.
(17) Bredol, M.; Jüstel, T.; Gutzov, S. *Opt. Mater*. **2001**, *18*, 337.
(18) (a) Bekiari, V.; Lianos, P.; Judenstein, P. *Chem. Phys. Lett.* **1999**, *307*, 310. (b) Moleski, R.; Stathatos, E.; Bekiari, V.; Lianos, P. *Thin Solid Films* **2002**, *416*, 279.
(19) (a) Franville, A.-C.; Zambon, D.; Mahiou, R.; Chou, S.; Troin, Y.; Cousseins, J. C. *J. Alloys Compd.* **1998**, *275−277*, 831. (b) Franville, A.-C.; Zambon, D.; Mahiou, R.; Troin, Y. *Chem. Mater.* **2000**, *12*, 428.
(20) (a) Fu, L. S.; Meng, Q. G.; Zhang, H. J.; Wang, S. B.; Yang, K. Y.; Ni, J. Z. *J. Phys. Chem. Solids* **2000**, *61*, 1877. (b) Liu, F.; Fu, L.; Meng, Q.; Li, H.; Guo, J.; Zhang, H. *New J. Chem.* **2003**, *27*, 233.
(21) Dong, D. W.; Jiang, S. C.; Men, Y. F.; Ji, X. L.; Jiang, B. Z. *Adv. Mater.* **2000**, *12*, 646.
(22) Bagwe, R. P.; Yang, C.; Hilliard, L. R.; Tan, W. *Langmuir* **2004**, *20*, 8336.
(23) Herrera, A. P.; Resto, O.; Briano, J. G.; Rinaldi, C. *Nanotechnology* **2005**, *16*, S618.
(24) Wang, F.; Beng Tan, W.; Zhang, Y.; Fan, X.; Wang, M. *Nanotechnology* **2006**, *17*, R1.
(25) (a) Lehn, J.-M. *Angew. Chem., Int. Ed.* **1990**, *29*, 1304. (b) Sá, G. F. de; Malta, O. L.; Mello Donegá, C. de; Simas, A. M.; Longo, R. L.; Santa-Cruz, P. A.; da Silva, E. F., Jr. *Coord. Chem. Rev* **2000**, *196*, 165.
(26) (a) Li, H.; Inoue, S.; Machida, K.; Adachi, G. *Chem. Mater.* **1999**, *11*, 3171. (b) Li, H.; Inoue, S.; Machida, K.; Adachi, G. *J. Lumin.* **2000**, *87−89*, 1069.
(27) Qiang, G. D.; Wang, M. Q.; Wang, M.; Fan, X. P.; Hong, Z. L. *J. Mater. Sci. Lett.* **1997**, *16*, 322.
(28) (a) Binnemans, K.; Lenaerts, P.; Driesen, K.; Gorller-Walrand, C. *J. Mater. Chem.* **2004**, *14*, 191. (b) Driesen, K.; Deun, R. V.; Gorller-Walrand, C.; Binnemans, K. *Chem. Mater.* **2004**, *16*, 1531. (c) Lenaerts, P.; Storms, A.; Mullens, J.; D'Haen, J.; Gorller-Walrand, C.; Binnemans, K.; Driesen, K. *Chem. Mater.* **2005**, *17*, 5194. (d) Binnemans, K. *Handbook on the Physics and Chemistry of Rare Earths*; Elsevier: Amsterdam, 2005; Vol. 34, Chapter 225, pp 107−225.
(29) Rosa, I. L. V.; Serra, O. A.; Nassar, E. J. *J. Lumin.* **1997**, *72−74*, 532.
(30) Lima, P. P.; Sá Ferreira, R. A.; Freire, R. O.; Paz, F. A. A.; Fu, L.; Alves, S., Jr.; Carlos, L. D.; Malta, O. *Chem. Phys. Chem.* **2006**, *7*, 735.
(31) Molina, C.; Dahmouche, K.; Messadeq, Y.; Ribeiro, S. J. L.; Silva, M. A. P.; de Zea Bermudez, V.; Carlos, L. D. *J. Lumin.* **2003**, *104*, 93.
(32) Nassar, E. J.; Serra, O. A.; Callefi, P. S.; Manso, C. M. C. P.; Neri, C. R. *Mater. Res.* **2001**, *4*, 18.
(33) Li, H. R.; Zhang, H. J.; Lin, J.; Wang, S. B.; Yang, K. Y. *J. Non-Cryst. Solids* **2000**, *278*, 218.
(34) Tanner, P. A.; Yan, B.; Zhang, H. *J. Mater. Sci.* **2000**, *35*, 4325.
(35) Nunes, S. C.; de Zea Bermudez, V.; Silva, M. M.; Smith, M. J.; Morales, E.; Carlos, L. D.; Sá Ferreira, R. A.; Rocha, J. *J. Solid State Electrochem.* **2006**, 10, 203.

prostheses and containers for sustained drug delivery.[36−38] Hybrids composed of PCL with an average molecular weight of 2000 g mol^{-1} have been also proposed as degradable bioglasses, coating materials for bone implants and prosthetic devices, supports for enzyme immobilization[39] and bone substitutes.[40] No references to the use of PCL hybrid host structures for the development of materials for optics have, however, been found. Thus, to the best of our knowledge, this is the first time that the PCL(530)/siloxane framework is considered as a candidate for the production of environmentally friendly luminescence biohybrid materials. Such materials may be expected to have lower environmental impact than that those currently used in commercial devices. Moreover, as in the PCL(530)/siloxane matrix both ends of the polymer chains are bonded to the inorganic network by means of urethane groups, this host structure may be viewed as a diurethanesil. Consequently, the present work will allow us to enlarge the investigation on the diurethanesil hybrids, which has been restricted to poly(oxyethylene) (POE)/siloxane systems.[41] The replacement of the POE chains by PCL(530) chains is of interest, because we have extensively demonstrated that in the lanthanide-doped diurea/diurethane cross-linked POE/siloxane systems (diureasils/diurethanesils), the coordinating ability of the matrix itself (provided by the carbonyl oxygen atoms of the urea/urethane groups and the ether oxygen atoms of the POE chains) plays a key role in the optical features of the materials, protecting the emitting species from deleterious quenching effects associated with water molecules.[41,42]

Results and Discussion

Complex Characterization. The analysis of several critical bands of the Fourier transform infrared (FT-IR) spectra of $Eu(tta)_3(H_2O)_2$ and $Eu(tta)_3$phen is useful for inspecting the composition of the first coordination sphere of the lanthanide ion. The strong broad band found at 3351 cm^{-1} in the FT-IR spectrum of the aquocomplex, associated with the stretching vibration mode of the OH groups of the water ligands, is missing in the FT-IR spectrum of the Eu-$(tta)_3$phen complex (see Figure S1 of the Supporting Information). In the latter spectrum, the feature due to the C−N stretching vibration mode (νC−N) of the free phen ligand is shifted, as expected, from 1643 to 1622 cm^{-1} (see Figure S1 of the Supporting Information).[43] In both cases, the event ascribed to the C═O stretching vibration mode (νC═O) of the free tta^- ligand is displaced from 1660 to 1600 cm^{-1} (see Figure S1 of the Supporting Information).[43] These results confirm the absence of water ligands and the presence of the phen ligand in the Eu^{3+} coordination sphere of the Eu-$(tta)_3$phen complex.

Table 1. Relevant Data of the $Eu(tta)_3(H_2O)_2$ and $Eu(tta)_3$phen Complexes

compd	λ_{max}(abs)[a] (nm)	λ_{max}(em) (nm)	IE (eV)	EA (eV)
$Eu(tta)_3(H_2O)_2$	340	271	5.3	3.6
$Eu(tta)_3$phen	340	265	5.2	3.6

[a] Measured in ethanol.

The $Eu(tta)_3(H_2O)_2$ and $Eu(tta)_3$phen complexes exhibit their lowest-energy absorption maxima at about 340 nm (see Figure S2 of the Supporting Information and Table 1). This common band corresponds to ligand singlet-to-singlet transitions and is thus associated with the tta^- ligands.[44] In both cases, the low-energy absorption edge is located near 400 nm (see Figure S2 of the Supporting Information). The aquocomplex displays another equally strong absorption band at about 271 nm (see Figure S2 of the Supporting Information and Table 1). Below 310 nm, the spectrum of $Eu(tta)_3$phen, dominated by an intense band centered at 265 nm, receives the contribution of the intraligand $\pi-\pi^*$ transitions of the two ligands (see Figure S2 of the Supporting Information).

The electron affinity (EA) and ionization energy (IE) of the complexes, indicated in Table 1, were calculated on the basis of their oxidation and reduction potentials, measured by cyclic voltammetry, using the following equations[45]

$$\mathrm{IE} = E_{\mathrm{ox,in}} + 4.35 \quad (1)$$

$$E(\mathrm{HOMO}) = -\mathrm{IE} \quad (2)$$

$$\mathrm{EA} = E_{\mathrm{red,in}} + 4.35 \quad (3)$$

The oxidation and reduction potentials were deduced from the intersection of two curves, one corresponding to the onset potential and the other to the residual current of the voltammogram. The redox couple ferrocene/ferricenium ion (Fc/Fc^+) was used as an external standard. Its energy, with respect to the vacuum level, defined as zero, was estimated to be −4.8 eV.[46] IE and EA are the relevant energy levels (HOMO and LUMO, respectively) for charge injection when such materials are used in light-emitting devices. The similarity of IE and EA values for $Eu(tta)_3(H_2O)_2$ and Eu-$(tta)_3$phen (Table 1), along with the observation of the same lowest-energy absorption maximum, indicate that the HOMO and LUMO energies of both complexes are essentially determined by the tta^- ligand.

The differential scanning calorimetry (DSC) and thermogravimetic analysis (TGA) curves of the complexes are reproduced in Figure 1. In the 100−115 °C temperature

(36) Pak, J.; Ford, J. L.; Rostron, C.; Walters, V. *Pharm. Acta Helv.* **1985**, *60*, 160.
(37) Grijpma, D. W.; Zondervan, G. J.; Penning, A. J. *J. Polym. Bull.* **1991**, *25*, 327.
(38) Coombes, A. G. A.; Rizzi, S. C.; Williamson, M.; Barralet, J. E.; Downes, S.; Wallace, W. A. *Biomaterials* **2004**, *25*, 315.
(39) Tian, D.; Dubois, Ph.; Jérôme, R. *Polymer* **1996**, 37, 17, 3983.
(40) Rhee, S-H.; Choi, J-H.; Kim, H.-M. *Biomaterials* **2002**, *23*, 4915.
(41) (a) Gonçalves, M. C.; de Zea Bermudez, V.; Sá Ferreira, R. A.; Carlos, L. D.; Ostrovskii, D.; Rocha, J. *Chem. Mater.* **2004**, *16*, 2530. (b) Gonçalves, M. C.; Silva, N. J. O.; de Zea Bermudez, V.; Sá Ferreira, R. A.; Carlos, L. D.; Dahmouche, K.; Santilli, C. V.; Ostrovskii, D.; Correia Vilela, I. C.; Craievich, A. F. *J. Phys. Chem. B* **2005**, *109*, 20093.
(42) (a) de Zea Bermudez, V.; Sá Ferreira, R. A.; Carlos, L. D.; Molina, C.; Dahmouche, K.; Ribeiro, S. J. L. *J. Phys. Chem. B* **2001**, *105* , 3378. (b) Dahmouche, K.; Carlos, L. D.; de Zea Bermudez, V.; Sá Ferreira, R. A.; Santilli, C. V.; Craievich, A. F. *J. Mater. Chem.* **2001**, *11*, 3249. (c) Sá Ferreira, R. A.; Carlos, L. D.; Gonçalves, R. R.; Ribeiro, S. J. L.; de Zea Bermudez, V. *Chem. Mater.* **2001**, *13* , 2991.
(43) Jablonski, Z.; R.-Himmel, I.; Dyrer, M. *Spectrochim. Acta* **1978**, *35A*, 1297.
(44) Silva, F. R. G.; Menezes, J. F. S.; Rocha, G. B.; Alves, S.; Brito, H. F.; Longo, R. L.; Malta, O. L. *J. Alloys Compd.* **2000**, *303−304*, 364.
(45) Al-Ibrahim, M.; Roth, H.-K.; Zhokhavets, U.; Gobsch, G.; Sensfuss, S. *Sol. Energy Mater. Sol. Cells* **2005**, *13*, 85.
(46) Pommerehne, J.; Vestweber, H.; Guss, W.; Mahrt, R. F.; Bässler, H.; Porsh, M.; Daub, J. *Adv. Mater.* **1995**, *7*, 551.

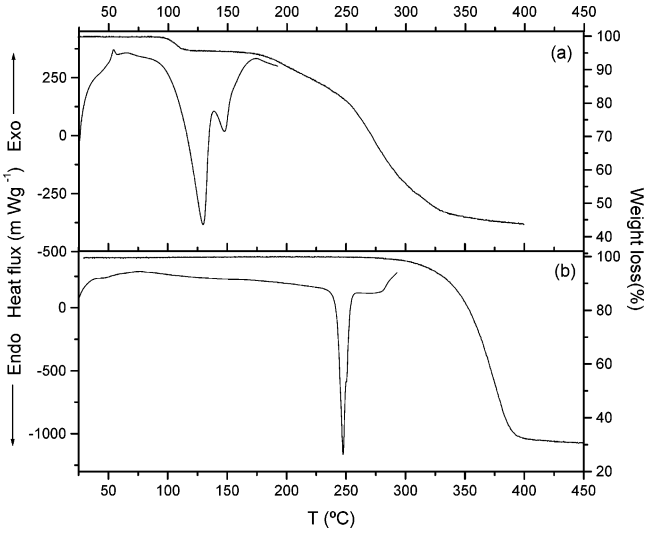

Figure 1. DSC (left axis) and TGA (right axis) curves of the (a) $Eu(tta)_3(H_2O)_2$ and (b) $Eu(tta)_3phen$ complexes.

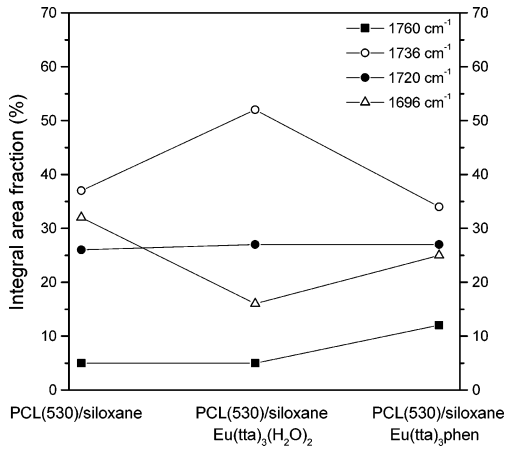

Figure 2. Integral intensity of the different spectral components resolved in the 1850−1650 cm^{-1} region of the nondoped PCL(530)/siloxane hybrid and the PCL(530)/siloxane-based hybrids incorporating $Eu(tta)_3(H_2O)_2$ and $Eu(tta)_3phen$.

range, the TGA curve of $Eu(tta)_3(H_2O)_2$ (Figure 1a) displays a mass loss of 5% that corresponds to the release of the two water molecules from the coordination sphere of the Eu^{3+} ion. In the corresponding DSC trace, this effect is manifested as an intense endothermic peak centered around 130 °C (onset at about 100 °C; Figure 1a). The weaker endotherm centered at 150 °C (onset at about 125 °C) in the same curve is associated with the melting of the complex (Figure 1a).[28d] At temperatures higher than approximately 180 °C, complex decomposition takes place (Figure 1a).

The DSC and TGA curves of $Eu(TTA)_3phen$ demonstrate the anhydrous character of this complex (Figure 1b). The sharp endotherm centered at about 245 °C (onset at approximately 240 °C) corresponds to the fusion of $Eu(tta)_3phen$ (Figure 1(b)). We note that the replacement of the two water ligands of $Eu(tta)_3(H_2O)_2$ by the phen ligand is clearly advantageous, as it imparts a thermal stability to the $Eu(tta)_3phen$ compound. The degradation of this complex begins only above 300 °C (Figure 1b).

Hybrid Characterization. In an attempt to get insight into the role played by the urethane carbonyl oxygen atoms and the PCL(530) ester carbonyl oxygen atoms in the coordination of the Eu^{3+} ions in the doped samples, we decided to inspect the FT-IR signatures of PCL(530)/siloxane/$Eu(tta)_3(H_2O)_2$ and PCL(530)/siloxane/$Eu(tta)_3phen$ in the spectral region typically associated with the stretching vibration of the carbonyl groups and compare them with that of the nondoped PCL(530)/siloxane matrix.

The "amide I" modes of urethane groups, which receive a major contribution from the carbonyl stretching vibration, appear between 1800 and 1600 cm^{-1}.[41] As these modes are sensitive to the specificity/magnitude of hydrogen-bonding modes,[47] in general the "amide I" band consists of several distinct components that correspond to different C═O environments usually known as associations. In the same spectral interval, the carbonyl stretching modes of the ester carbonyl groups give rise to bands that have been widely explored for crystallinity determination.[48,49]

Rich information may be retrieved from the carbonyl stretching region of the nondoped matrix (see Figure S3 of the Supporting Information). Curve-fitting procedures performed in the 1800−1650 cm^{-1} interval allowed us to resolve the band profile of the PCL(530)/siloxane hybrid into four distinct components located at about 1762, 1736, 1720, and 1692 cm^{-1} (see Figure S4 of the Supporting Information). The weak 1762 cm^{-1} band is associated with the presence of "free" (non-hydrogen-bonded) carbonyl groups of the urethane cross-links (Scheme 2A).[50] The 1736 cm^{-1} component is characteristic of amorphous PCL(530) chains.[48,49] The component found at 1720 cm^{-1} is attributed to the presence of hydrogen-bonded oxyethylene/urethane associations (Scheme 2B).[50] Finally, the 1692 cm^{-1} feature is assigned to the formation of urethane−urethane hydrogen-bonded associations (Scheme 2C).[50] Because of their structural similarity, it is, however, very likely that associations such as that represented in Scheme 2D also absorb at 1692 cm^{-1}.

In spite of the low concentration of europium in the samples prepared (see Experimental Section), doping the PCL(530)/siloxane hybrid matrix with $Eu(tta)_3(H_2O)_2$ and $Eu(tta)_3phen$ modifies the carbonyl stretching region of the matrix, leading to band redistribution (see Figures S3 and S4 of the Supporting Information). Upon incorporation of $Eu(tta)_3phen$, the intensity maximum of the band profile is shifted from about 1733 to 1726 cm^{-1} (see Figure S3 of the Supporting Information).

The plot of Figure 2 reveals that the addition of $Eu(tta)_3(H_2O)_2$ has more dramatic consequences on the chemical environment of the carbonyl groups than $Eu(tta)_3phen$. In the case of $Eu(tta)_3(H_2O)_2$ doping, a significant breakdown of the hydrogen-bonded associations responsible for the 1692 cm^{-1} component (i.e., urethane/urethane associations and urethane/ester carbonyl associations) occurs. In parallel, the proportion of ester carbonyl groups increases dramatically.

(47) Skrovanek, D. J.; Howe, S. E.; Painter, P. C.; Coleman, M. M. *Macromolecules* **1985**, *18*, 1676.
(48) He, Y.; Inoue, Y. *Polym. Int.* **2000**, *49*, 623.
(49) Sanchis, A.; Prolongo, M. G.; Salom, C.; Masegosa, R. M. *J. Polym. Sci., Part B: Polym. Phys.* **1979**, *17*, 837.
(50) de Zea Bermudez, V.; Ostrovskii, D.; Gonçalves, M. C.; Carlos, L. D.; Sá Ferreira, R. A.; Reis, L.; Jacobsson, P. *Phys. Chem. Chem. Phys.* **2004**, *6*, 638.

Scheme 2. Tentative Representation of the Chemical Environment of the Carbonyl Groups in the PCL (530)/Siloxane Hybrid Host Matrix

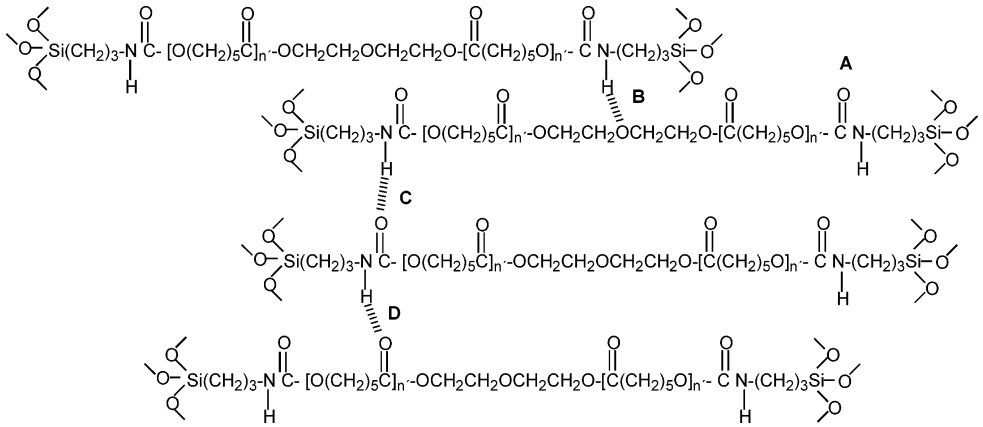

The fraction of oxyethylene/urethane associations and the population of "free" urethane groups remains constant, however (Figure 2). Typically, when urethane/urethane associations are destroyed, the number of "free" carbonyl groups tends to increase and/or new hydrogen-bonded associations are formed.[50] As this is not the case here, we propose that the hydrogen-bonded associations destroyed in the PCL(530)/siloxane/Eu(tta)$_3$(H$_2$O)$_2$ sample are essentially the urethane/ester carbonyl ones. We emphasize that the rupture of these associations frees ester carbonyl groups without increasing the number of available "free" urethane groups (Scheme 2D), leaving the oxyethylene/urethane associations unperturbed.

Although the addition of Eu(tta)$_3$phen to PCL(530)/siloxane does not produce such marked effects (Figure 2), we observe a slight rupture of the urethane/urethane associations, whereas the proportion of urethane/ester carbonyl and oxyethylene/urethane associations remains practically the same. At the same time, the fraction of "free" urethane groups rises.

These findings suggest that the inclusion of Eu(tta)$_3$(H$_2$O)$_2$ within the PCL(530)/siloxane medium promotes the interaction of the complex (i.e., of the Eu^{3+} ions) specifically with the carbonyl groups of the PCL(530) chains of the hybrid host. This explanation apparently eliminates the contribution of the urethane carbonyl oxygen atoms to the coordination process of the Eu^{3+} ions. Typically, in mono-[50]/diurethanesils[41] and diureasils,[30,51] the coordination of lanthanide ions (introduced as a triflate salt[41,50] and as a complex,[30,51] respectively) to the carbonyl oxygen atoms of the urethane and urea cross-links of the hybrid matrix, respectively, is easily monitored in the amide I region through the detection of a new event emerging below the component at approximately 1690 cm^{-1}. In the carbonyl stretching region of the PCL(530)/siloxane/Eu(tta)$_3$(H$_2$O)$_2$ material, this Eu^{3+} coordination-sensitive feature is not seen (see Figure S3 of the Supporting Information). However, it is possible that the concentration of Eu^{3+} is too low to yield a detectable band by FT-IR. We recall that the concentration of Eu^{3+} in PCL(530)/siloxane/Eu(tta)$_3$(H$_2$O)$_2$ (Si/Eu = 19 g/g) is lower than the minimum concentration for which this Eu^{3+} coordination-sensitive absorption is identified by FT-IR in the case of the europium triflate-doped diurethanesils[41] and the Eu(nta)$_3$bpy -doped diureasils (where nta is 1-(2-naphthyl)-4,4,4-trifluoro-1,3-butanedionate and bpy is 2,2′-bipyridine)[51] (Si/Eu = 3.5[41] and 7.9 g/g,[51] respectively). Furthermore, the possibility that a new band is masked by the broad component centered at 1690 cm^{-1} cannot be discarded either (see Figure S4 of the Supporting Information).

The data obtained also indicate that, unlike Eu(tta)$_3$(H$_2$O)$_2$, whose interaction with the PCL(530)/siloxane host appears to be restricted to the environment of the urethane/ester carbonyl associations, Eu(tta)$_3$phen exerts its influence essentially on the urethane−urethane associations of the PCL(530)/siloxane structure, weakening them. Considering the bulkiness of the ligands in the latter complex, we consider that this breakdown of the hydrogen bonds is consistent with the existence of steric constraints. However, the arguments presented above for the PCL(530)/siloxane/Eu(tta)$_3$(H$_2$O)$_2$ material regarding the formation of new associations characteristic of Eu^{3+}/carbonyl bonding apply here as well, as the concentration of Eu^{3+} in PCL(530)/siloxane/Eu(tta)$_3$phen (Si/Eu = 24 g/g) is slightly lower than that of Eu(tta)$_3$(H$_2$O)$_2$ in the same hybrid host matrix.

The DSC curves of the doped PCL(530)/siloxane hybrids exhibit a very weak endotherm in the low-temperature range (Figure 3). This event is centered at 47 °C (onset at about 42 °C) in the case of Eu(tta)$_3$(H$_2$O)$_2$ doping (Figure 3a) and at 36 °C (onset at about 29 °C) in the case of Eu(tta)$_3$phen doping (Figure 3b). It is of interest to mention that, although the parent PCL(530) organic precursor is crystalline (the reported melting temperature of this compound is 36−48 °C), the nondoped PCL(530)/siloxane matrix is totally amorphous.[35] Thus the weak endothermic event observed in the thermograms of PCL(530)/siloxane/Eu(tta)$_3$(H$_2$O)$_2$ and PCL(530)/siloxane/Eu(tta)$_3$phen may be associated with the fusion of short uncomplexed polymer segments of the PCL(530)/siloxane hybrid host. Considering that the reported value for the bulk enthalpy of melting of PCL (i.e., 100% crystalline) ΔH_m^0 is 166.7 J g^{-1},[52] the proportion of crystal-

(51) Fu, L.; Sá Ferreira, R. A.; Silva, N. J. O.; Fernandes, A. J.; Ribeiro-Claro, P.; Gonçalves, I. S.; de Zea Bermudez, V.; Carlos, L. D. *J. Mater. Chem*. **2005**, *15*, 3117.

(52) Chen, H.-L.; Li, L.-J., Lin, T.-L. *Macromolecules* **1998**, *31*, 2255.

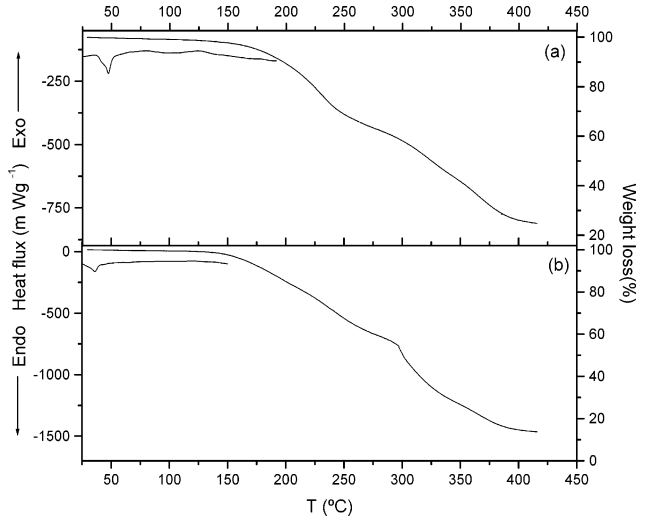

Figure 3. DSC (left axis) and TGA (right axis) curves of the PCL(530)/siloxane-based hybrids incorporating (a) $Eu(tta)_3(H_2O)_2$ and (b) $Eu(tta)_3$phen complexes.

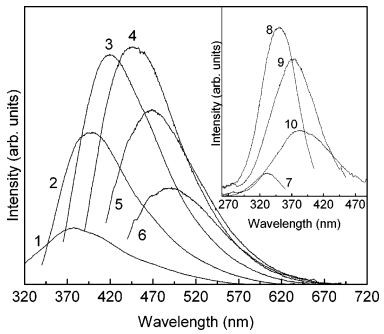

Figure 4. Emission spectra of the PCL(530)/siloxane hybrid host excited at (1) 300, (2) 325, (3) 350, (4) 375, (5) 400, and (6) 425 nm. The inset shows the excitation spectra monitored at (7) 380, (8) 420, (9) 470, and (10) 510 nm.

linity in the PCL(530)/siloxane/$Eu(tta)_3(H_2O)_2$ ($\Delta H_m = 3.1$ J g^{-1}) and PCL(530)/siloxane/$Eu(tta)_3$phen ($\Delta H_m = 2.5$ J g^{-1}) samples is 1.9 and 1.5%, respectively.

It is noteworthy that the pair of peaks ascribed to the two water ligands of the aquocomplex are absent in the DSC thermogram of PCL(530)/siloxane/$Eu(tta)_3(H_2O)_2$ (Figure 3a). No mass loss associated with the removal of the two water molecules is detected by TGA (Figure 3a). The TGA curves of the two hybrid samples reveal that both materials start to decompose at approximately 200 °C.

The PCL(530)/siloxane hybrid host is photoluminescent prior to the incorporation of the Eu^{3+}-based complexes. As shown in Figure 4, the emission spectra of the PCL(530)/siloxane hybrid host are composed of a large broad band, whose peak position deviates to the red as the excitation wavelength increases. These emission features resemble those previously reported for other amine functionalized hybrids, such as the diureasils/diurethanesils, and have been ascribed to electron−hole recombination occurring within oxygen-related defects present in the siliceous domains and within the urea/urethane groups.[10,53] The emission dependence on

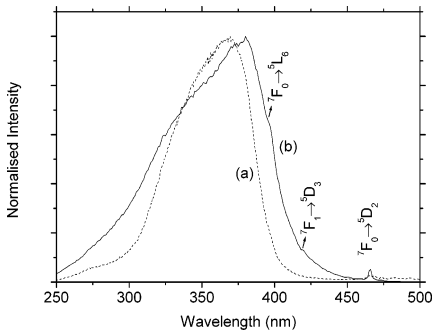

Figure 5. Excitation spectra of the (a) PCL(530)/siloxane/$Eu(tta)_3(H_2O)_2$ and (b) PCL(530)/siloxane/$Eu(tta)_3$phen hybrids monitored at 617 and 612 nm, respectively.

the excitation wavelength was recently modeled as radiative recombinations involving thermal relaxation within localized states, in the framework of the extended multiple trapping approach.[54] The excitation spectra were monitored along the broad emission band (inset of Figure 4), showing that the excited states of the PCL(530)/siloxane hybrid range from the UV (250 nm) to the blue spectral region (480 nm).

Figure 5 compares the excitation spectrum (monitored around the most intense $^5D_0 \rightarrow {}^7F_2$ emission transition) of the PCL(530)/siloxane/$Eu(tta)_3(H_2O)_2$ and PCL(530)/siloxane/$Eu(tta)_3$phen samples. Both spectra display a large broad band peaking at ∼370 and ∼380 nm, respectively, which may result from the overlap of the $\pi-\pi^*$ electron transition of the organic ligands[26a,44] and the excited states of the PCL(530)/siloxane hybrid (inset of Figure 4). In the excitation spectrum of the hybrid incorporating the $Eu(tta)_3$phen complex, it is also possible to discern the $^7F_0 \rightarrow {}^5L_6$, $^7F_1 \rightarrow {}^5D_3$ (taking into account the selection rules for forced electric-dipole transitions, $\Delta J = 2, 4, 6$, this is a more reasonable assignment at room temperature than $^7F_0 \rightarrow {}^5D_3$) and $^7F_0 \rightarrow {}^5D_2$ intra-4f^6 transitions (Figure 5). The absence or negligible intensity of the intra-4f^6 transitions in these excitation spectra indicates that the Eu^{3+} ions are mainly excited via an effective sensitized process involving the ligands excited states, rather than by direct intra-4f^6 excitation. Comparison of the PCL(530)/siloxane/$Eu(tta)_3(H_2O)_2$ excitation spectrum with that of the starting complex[55] allows us to infer that in the case of the complex, the broad band overlaps intra-4f^6 lines. Thus, the incorporation of the complex into the PCL(530)/siloxane hybrid host framework results in an improvement of the sensitization process. We will return to this point below.

The PCL(530)/siloxane//$Eu(tta)_3(H_2O)_2$ hybrid shows an intense red photoluminescence when irradiated with ultraviolet (UV) radiation (Figure 6). Figure 7A shows the emission spectra of the hybrids under the excitation wavelength that maximizes the Eu^{3+} emission. The spectra are composed of the characteristic sharp peaks of the Eu^{3+} $^5D_0 \rightarrow {}^7F_{0-4}$ transitions. Only a single line is observed for the nondegenerated $^5D_0 \rightarrow {}^7F_0$ transition (Figure 7B), with a

(53) (a) Carlos, L. D.; Sá Ferreira, R. A.; de Zea Bermudez, V.; Ribeiro, S. J. L. *Adv. Funct. Mater.* **2001**, *11*, 111. (b) Carlos, L. D.; Sá Ferreira, R. A.; Pereira, R. N.; Assunção, M.; de Zea Bermudez, V. *J. Phys. Chem. B* **2004**, *108*, 14924.

(54) (a) Sá Ferreira, R. A.; Ferreira, A. L.; Carlos, L. D. *Eur. Phys. J. B* **2006**, *50*, 371. (b) Sá Ferreira, R. A.; Ferreira, A. L.; Carlos, L. D. *J. Non-Cryst. Solids* **2006**, *352*, 1225.

(55) Teotonio, E. S.; Brito, H. F.; Felinto, M. C. F. C.; Kodaira, C. A.; Malta, O. L. *J. Coord. Chem.* **2003**, *56*, 10, 913.

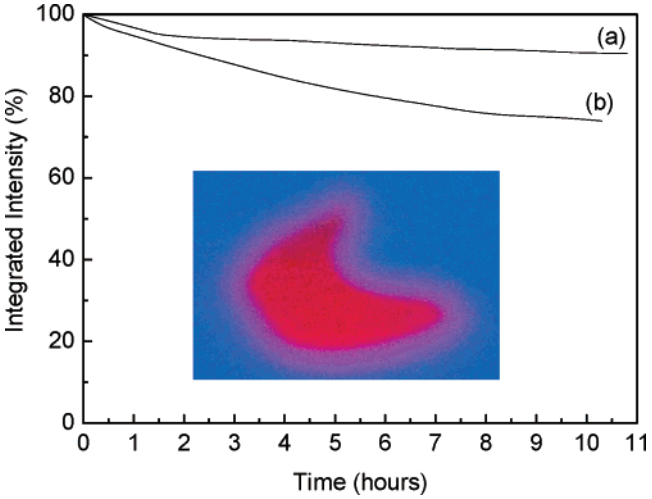

Figure 6. Emission intensity under UVA excitation as a function of exposure time for the (a) PCL(530)/siloxane/Eu(tta)$_3$(H$_2$O)$_2$ and (b) PCL(530)/siloxane/Eu(tta)$_3$phen hybrids under UV irradiation at 370 and 380 nm, respectively. The photography shows the PCL(530)/siloxane/Eu(tta)$_3$(H$_2$O)$_2$ hybrid under UV irradiation (366 nm).

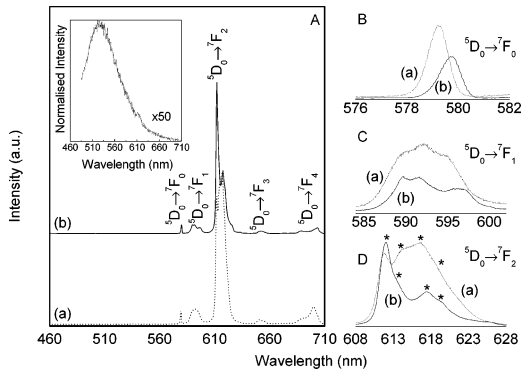

Figure 7. (A) Emission spectra of PCL(530)/siloxane/Eu(tta)$_3$(H$_2$O)$_2$ (a) and PCL(530)/siloxane/Eu(tta)$_3$phen (b) hybrids excited at 370 and 380 nm, respectively. The inset shows the emission spectra of the PCL(530)/siloxane/Eu(tta)$_3$(H$_2$O)$_2$ excited at 465 nm. (B−D) Details of the $^5D_0 \rightarrow {}^7F_{0-2}$ transitions. The asterisks identify the four distinctly discerned $^7F_2$ Stark components.

typical full-width at half-maximum (fwhm) value of ~20 cm^{-1}, suggesting that all Eu^{3+} ions occupy the same average chemical environment. Moreover, the energy, fwhm, and number of emission lines are independent of the selected excitation wavelength. The detection of a single line for the $^5D_0 \rightarrow {}^7F_0$ transition (Figure 7B), the local-field splitting of the $^7F_{1,2}$ levels into 3 and 4 Stark components (panels C and D in Figure 7, respectively) and the higher intensity of the $^5D_0 \rightarrow {}^7F_2$ transition indicate that the Eu^{3+} local coordination site has a low symmetry without an inversion center. For the PCL(530)/siloxane/Eu(tta)$_3$(H$_2$O)$_2$ hybrid, upon exciting along the broad band in Figure 5 (300−420 nm), no emission arising from the ligands triplet levels or from the PCL(530)/siloxane host was detected, pointing out an efficient energy transfer from PCL(530)/siloxane and the organic ligands to the Eu^{3+} ions. However, upon excitation of the hybrid around 465 nm, it is possible to discern a large broad band peaking at ca. 525 nm (inset of Figure 7A). This band was previously observed for emission of a Gd^{3+} analogue complex and was assigned to the emission arising from the triplet state localized in each tta$^-$ ligand.[55] For the latter excitation wavelength (465 nm, $^5D_2$ level), no emission from the Eu^{3+} ions resulted, indicating that the energy transfer channels resonant with the Eu^{3+} $^5D_2$ level are not efficient in populating the Eu^{3+} states. For the PCL(530)/siloxane/Eu(tta)$_3$phen hybrid, only the Eu^{3+} lines could be observed for excitation wavelengths ranging from 300 to 420 nm and under excitation into the $^5D_2$ level.

Comparing the Eu^{3+} emission features of the hybrids with those of the complexes, changes are observed in the energy and fwhm of the $^5D_0 \rightarrow {}^7F_{0-4}$ transitions, which points out an effective interaction between the Eu^{3+} ions and the PCL(530)/siloxane host. The increase in the fwhm for the hybrids also suggests a higher nonhomogeneous distribution of similar Eu^{3+} chemical environments due to changes outside the coordination polyhedron.[30] As recently suggested for the incorporation of other Eu^{3+} based complexes in amine cross-linked organic−inorganic hybrids, such alterations may be related to the essentially amorphous local structure of the host that accommodates in slightly different ways the Eu^{3+} first-coordination sphere, also leading to slight modifications in the phonon density distribution.[30]

The $^5D_0$ emission decay curves were monitored within the $^5D_0 \rightarrow {}^7F_2$ transition under the excitation wavelength that maximizes the emission intensity (not shown). The decay curves are well-reproduced by means of a single-exponential function, yielding $^5D_0$ lifetime values of 0.679 ± 0.001 ms and 0.622 ± 0.002 ms for PCL(530)/siloxane/Eu(tta)$_3$phen and PCL(530)/siloxane/Eu(tta)$_3$(H$_2$O)$_2$, respectively. Although the $^5D_0$ lifetime value for the PCL(530)/siloxane/Eu(tta)$_3$phen material is smaller than that reported for the isolated complex (0.976 ms[44]), the incorporation of the Eu(tta)$_3$(H$_2$O)$_2$ complex into the hybrid induces an increase in the $^5D_0$ lifetime value, with respect to that estimated for the isolated complex (0.34 ms[26a,55]).

On the basis of the luminescence data presented above (i.e., emission spectra and $^5D_0$ lifetimes), it is possible to estimate the $^5D_0$ radiative (k_r) and nonradiative (k_{nr}) transition probabilities and the $^5D_0$ quantum efficiency (q) of the hybrids. Assuming that only nonradiative and radiative processes are involved in the depopulation of the $^5D_0$ state, q may be defined as

$$q = \frac{k_r}{k_r + k_{nr}} \tag{4}$$

The emission intensity (I) taken as the integrated intensity S of the emission curves for the $^5D_0 \rightarrow {}^7F_{0-4}$ transitions is expressed by

$$I_{i\rightarrow j} = \hbar w_{i\rightarrow j} A_{i\rightarrow j} N_i \equiv S_{i\rightarrow j} \tag{5}$$

where i and j represent the initial ($^5D_0$) and final ($^7F_{0-4}$) levels, respectively, $\hbar w_{i\rightarrow j}$ is the transition energy, $A_{i\rightarrow j}$ corresponds to Einstein's coefficient of spontaneous emission, and N_i is the population of the $^5D_0$ emitting level.[56]

The radiative contribution may be calculated from the relative intensities of the $^5D_0 \rightarrow {}^7F_{0-4}$ transitions. The

(56) Carlos, L. D.; Messaddeq, Y.; Brito, H. F.; Sá Ferreira, R. A.; de Zea Bermudez, V.; Ribeiro, S. J. L. *Adv. Mater.* **2000**, *12*, 594.
(57) Werts, M. H. V.; Jukes, R. T. F.; Verhoeven, J. W. *Phys. Chem. Chem. Phys.* **2002**, *4*, 1542.

Table 2. $^5D_0$ Lifetime (τ), Radiative (k_r) and Nonradiative (k_{nr}) Transition Probabilities, and Quantum Efficiency (q) Values and Maximum Quantum Yield (η) for the Isolated $Eu(tta)_3(H_2O)_2$ and $Eu(tta)_3$phen Complexes and Incorporated into Several Hybrid Hosts. The data were obtained at room temperature.

host	τ (ms)	k_r (ms^{-1})	k_{nr} (ms^{-1})	q (%)	η (%)	ref
			$Eu(tta)_3(H_2O)_2$			
	0.34	0.806	2.137	27		31
	0.3	1.110	2.736		29	55
PCL(530)/siloxane	0.622	0.595	1.013	37	13	
diureasil	0.57	1.299	0.476	74		31
epoxy resin	0.442	1.034	1.229	46		59
			$Eu(tta)_3$phen			
	0.976				69	44
PCL(530)/siloxane	0.679	0.651	0.822	44	22	
merrifield resin	0.500				22	58a
TMOS-DEDMS[a]	0.590				27	28c,58b
TMOS-GLYMO[a]	0.600				34	28c,58b

[a] Samples processed as thin films.

branching ratio for the $^5D_0 \rightarrow {}^7F_{5,6}$ transitions must be neglected because of their poor relative intensity with respect to that of the remaining $^5D_0 \rightarrow {}^7F_{0-4}$ transitions. Their influence on the depopulation of the $^5D_0$ excited state can therefore be ignored. The $^5D_0 \rightarrow {}^7F_1$ transition can be considered as a reference because of its dipolar magnetic nature, so k_r can be calculated as

$$k_r = A_{0\rightarrow 1}\frac{\hbar\omega_{0\rightarrow 1}}{S_{0\rightarrow 1}}\sum_{J=0}^{4}\frac{S_{0-J}}{\hbar\omega_{0-J}} \quad (6)$$

where A_{0-1} is Einstein's coefficient of spontaneous emission between the $^5D_0$ and the $^7F_1$ Stark levels.

The $^5D_0 \rightarrow {}^7F_1$ transition does not depend on the local ligand field seen by Eu^{3+} ions and thus may be used as a reference for the whole spectrum; in vacuum, $A_{0-1} = 14.65$ s^{-1}.[53] An effective refractive index of 1.5 was used, leading to $A(^5D_0 \rightarrow {}^7F_1) \approx 50$ s^{-1}. The values found for q (%), k_r (ms^{-1}), and k_{nr} (ms^{-1}) for PCL(530)/siloxane/$Eu(tta)_3$phen and PCL(530)/siloxane/$Eu(tta)_3(H_2O)_2$, are shown in (Table 2).

The absolute emission quantum yields estimated for PCL(530)/siloxane/$Eu(tta)_3$phen and PCL(530)/siloxane/$Eu(tta)_3(H_2O)_2$ are 22 and 13%, respectively (Table 2). In common with the situation observed for the q values, the higher value found for the former hybrid may be caused by the higher nonradiative transition probability (k_{nr}) of the PCL(530)/siloxane/$Eu(tta)_3(H_2O)_2$.

It is useful to compare the above results with those reported in the literature for the isolated $Eu(tta)_3$phen complex. The previously reported data for this complex refer to the estimation of the overall emission quantum yield (ϕ) that has been theoretically and experimentally determined as being 63 and 69%, respectively.[55] The lower value found for the PCL(530)/siloxane/$Eu(tta)_3$phen hybrid leads us to conclude that the $^5D_0$ nonradiative paths in the PCL(530)/siloxane/$Eu(tta)_3$phen hybrid are higher than those existent in the $Eu(tta)_3$phen complex. As the absolute emission quantum yield is defined as the ratio between the number of emitted and absorbed photons, then $\phi \leq q$. We are thus led to conclude that the $^5D_0$ nonradiative paths in the PCL(530)/siloxane/$Eu(tta)_3$phen hybrid are higher than those existent in the $Eu(tta)_3$phen complex. The same conclusion may be derived from the analysis of the $^5D_0$ lifetime and quantum yield values of other systems based on the $Eu(tta)_3$phen complex and other organic−inorganic hybrid hosts, such as the Merrifield resin,[58a] tetramethoxysilane (TMOS)-diethoxydimethylsilane (DEDMS) and TMOS-3-glycidoxypropyltrimethosysilane (GLYMO),[28c,58b] as shown in Table 2. For all these materials, a decrease in the $^5D_0$ lifetime and in the emission quantum yield values is observed after complex incorporation, suggesting the appearance of nonradiative channels that were not present in the isolated complex.

The q value reported for the isolated $Eu(tta)_3(H_2O)_2$ complex (∼27%[31]) reveals that the complex incorporation into the PCL(530)/siloxane host contributes to enhance the $^5D_0$ quantum efficiency. The increase in the q value may be attributed to a decrease in the k_{nr} value in the hybrid with respect to that of the complex (2.736 m s^{-1} [55]). The k_{nr} decreases very likely originated from the replacement of the water molecules (i.e., OH oscillators) present in the Eu^{3+} first-coordination sphere of the starting complex by oxygen atoms of the carbonyl groups of the PCL(530)/siloxane host. We will return to this point below. Nevertheless, the absolute emission quantum of the PCL(530)/siloxane/$Eu(tta)_3(H_2O)_2$ hybrid is lower (13%) than that of the isolated complex (29%[55]), indicating that the UV absorption and energy transfer phenomena are less efficient in the hybrid.

The $Eu(tta)_3(H_2O)_2$ complex is among the most studied β-diketonates complexes, and has been already incorporated into other organic−inorganic hosts, such as, for instance, the diureasils,[31] and polymer resins.[58a,59] Table 2 compares the $^5D_0$ lifetime, k_r, k_{nr}, and q values and quantum yields reported for these materials with those estimated for the PCL(530)/siloxane hybrid. In the case of the $Eu(tta)_3(H_2O)_2$ complex, an increase in k_r and a decrease in k_{nr} occurs when the $Eu(tta)_3(H_2O)_2$ complex is incorporated into the diureasil matrix and into the polymer resin, leading to higher q values (74%[31] and (46%)[59]respectively) than those resulting from its incorporation into the PCL/siloxane hybrid host. These differences are induced by the different chemical environments experienced by the complex in the three organic−inorganic hosts. In particular, for the diureasil and the epoxy resin, the local interaction between the complex and the hybrid host occurs through the oxygen atoms of the polymer chains,[31,59] whereas in the case studied here, the complex interacts with the host matrix via the oxygen atoms of the carbonyl groups of the hybrid structure. In all cases, the removal of water molecules from the Eu^{3+} first-coordination sphere might happen, inducing the increase in the quantum yield and efficiency values.

The removal of water molecules from the Eu^{3+} coordination sphere after incorporation into the PCL(530)/siloxane may be further studied. On the basis of the empirical formula

(58) (a) Lenaerts, P.; Driesen, K.; Van Deun, R.; Binnemans, K. *Chem. Mater*. **2005**, *17*, 2148. (b) Lenaerts, P.; Ryckebosch, E.; Driesen, K.; Van Deun, R.; Nockemann, P.; Görller-Walrand, C.; Binnemans, K. *J. Lumin*. **2005**, *114*, 77.

(59) (a) Parra, D. F.; Mucciolo, A.; Brito, H. F.; Thompson, L. C. *J. Solid State Chem*. **2003**, *171*, 412. (b) Parra, D. F.; Brito, H. F.; Matos, J. R.; Carlos, L. D. *J. Appl. Polym. Sci*. **2002**, *83*, 2716.

suggested by Supkowski and Horrocks,[60] we are able to estimate the number of water molecules (n_w) coordinated to the metal ion in the PCL hybrid host with the following formula

$$n_w = 1.11 \times \lfloor k_{exp} - k_r - 0.31 \rfloor \quad (7)$$

where k_{exp} is the reciprocal value of the $^5D_0$ lifetime.

On the basis of eq 7, we estimated that in the case of PCL-(530)/Eu(tta)$_3$(H$_2$O)$_2$ 0.8 ± 0.1 water molecules are coordinated to the Eu^{3+} ions. This finding leads us to deduce that at least one water molecule of the Eu(tta)$_3$(H$_2$O)$_2$ complex was removed from the Eu^{3+} first coordination shell after being added to the PCL(530)/siloxane host. The removal of water molecules from Eu^{3+} ion first-coordination sphere in the Eu(tta)$_3$(H$_2$O)$_2$ complex was also detected in other hosts, such as the diureasil,[31] TMOS-DEDMS, and TMOS-GLYMO[58b] organic−inorganic hybrids, and is in complete accordance with the FT-IR analyses proposed above.

Recently, it was demonstrated that amine-based organic−inorganic hybrids contribute to the photostability of β-diketonate complexes.[30] The photostability of the [Eu(btfa)$_3$-(4,4′-bpy)(EtOH)] complex (where 4,4′-bpy is 4,4′-bipyridine, btfa is 4,4,4-trifluoro-1-phenyl-1,3-butanedione, and EtOH is ethanol) was significantly improved after incorporating the complex into a diureasil hybrid, the resulting material displaying ∼100% photostability under UVA radiation.[30] To evaluate the photostability of the PCL/siloxane-based hybrids examined in the present work, we monitored the integrated intensity of the $^5D_0 \rightarrow {}^7F_{0-4}$ transitions in real time as a function of the exposure time for the excitation wavelength that maximizes their emission intensity, namely 370 and 380 nm (UVA) for PCL(530)/siloxane/Eu(tta)$_3$(H$_2$O)$_2$ and PCL-(530)/siloxane/Eu(tta)$_3$phen, respectively (Figure 5). Under UVA exposure, the PCL(530)/siloxane/Eu(tta)$_3$phen hybrid emission intensity decreases around 25% in 11 h, whereas in the case of PCL(530)/siloxane/Eu(tta)$_3$(H$_2$O)$_2$, an emission intensity degradation of 10% in 11 h is discerned (Figure 6). It the latter material, 5% of emission intensity degradation takes place in the first 2 h of exposure. These results show that the PCL(530)/siloxane hybrid host has a higher contribution to the photostability of the Eu(tta)$_3$(H$_2$O)$_2$ complex than that of the Eu(tta)$_3$phen complex. This observation is in good agreement with the more effective interaction being between the hybrid and the Eu(tta)$_3$(H$_2$O)$_2$ complex rather than with the same hybrid and the Eu(tta)$_3$phen complex. This aspect is probably associated with the higher interaction that exists between the Eu(tta)$_3$(H$_2$O)$_2$ complex and the PCL-(530)/siloxane host (via the replacement of one water molecule in the Eu^{3+} first-coordination sphere by the oxygen atom of a carbonyl group of the hybrid host), when compared with that observed in the case of the Eu(tta)$_3$phen complex.

Experimental Section

Thenoyltrifluoracetone (Htta, Aldrich, 99%), europium chloride ($EuCl_3$·6H$_2$O, Aldrich, 99%), 1,10-phenanthroline (phen, Aldrich, +99%), α,ω-hydroxyl poly(ϵ-caprolactone) (PCL(530), Fluka, average molecular weight 530 g/mol), and 3-isocyanatepropyltriethoxysilane (ICPTES, Fluka, 95%) were used as received. Ethanol (CH_3CH_2OH, Merck, PA grade) and tetrahydrofuran (THF; Merck, puriss. PA grade) were stored over molecular sieves. High-purity distilled water was used in all experiments.

The europium complexes were prepared using the conventional method described in detail elsewhere:[61] (a) Synthesis of Eu(tta)$_3$-(H$_2$O)$_2$. A mass of 0.6670 g (3 mmol) of Htta was dissolved in 15 mL of CH_3CH_2OH. The pH of this solution was adjusted to 6−7 by adding an appropriate amount of an aqueous NaOH solution (1 M). An aqueous solution of $EuCl_3$·6H$_2$O (0.3611 g, 1 mmol in 5 mL of water) was then added dropwise to the ethanolic solution of Htta. The addition of 100 mL of water on heating at 60 °C for 120 min followed. The resulting solution was left in the fume cupboard until precipitation. The yellow solid obtained was filtered off, washed with water and dried in a vacuum desiccator at room temperature. Yield: 81% Anal. Calcd: C, 33.83; H, 1.88. Found: C, 33.86; H, 1.79. (b) Synthesis of Eu(tta)$_3$phen. The preparation of this complex differed from that of Eu(tta)$_3$(H$_2$O)$_2$ only in the addition of a mass of 0.1861 g (1 mmol) of phen to the ethanolic solution of Htta Yield: 74% Anal. Calcd: C, 43.41; H, 2.00. Found: C, 43.37; H, 2.81.

The nondoped and doped hybrids were prepared according to a procedure described in detail elsewhere,[35] but using a different ICPTES:CH_3CH_2OH:H$_2$O molar ratio (here, 1:4:3). The synthesis of the host PCL(530)/siloxane hybrid involved two steps. In the first stage, a urethane cross-link was formed between the hydroxyl (−OH) end groups of the PCL(530) chain and the isocyanate (−N═C═O) groups of ICPTES in THF at 70−80 °C to yield the PCL-(530)/siloxane hybrid precursor. In the second stage, appropriate amounts of CH_3CH_2OH and water were added to this solution to promote the sol−gel characteristic reactions (i.e., hydrolysis and condensation). The complex was incorporated in the latter stage. In the PCL(530)/siloxane/Eu(tta)$_3$(H$_2$O)$_2$ and PCL(530)/siloxane/Eu(tta)$_3$phen hybrids prepared, the Si/Eu ratios are 19 g/g (105 mol/mol) and 24 g/g (130 mol/mol), respectively, and the [(C═O)(CH$_2$)$_5$O]/Eu ratios are 245 and 304 mol/mol, respectively.

Elemental analyses of the complexes were performed at Centro de Apoio Científico e Tecnolóxico á Investigación (CACTI)-University of Vigo (Spain).

The Fourier transform infrared (FT-IR) spectra were acquired at room temperature on a Unicam FT-IR spectrophotometer. The spectra were collected in the 4000−400 cm^{-1} range by averaging 120 scans at a resolution of 4 cm^{-1}. About 2 mg of each compound was mixed with potassium bromide (Merck, spectroscopic grade) finely ground and pressed into pellets. To evaluate complex band envelopes and identify underlying spectral components, we used the iterative least-squares curve-fitting procedure in the PeakFit[62] software throughout this study. The best fit of the experimental data was obtained by varying the frequency, bandwidth, and intensity of the bands and using a Gaussian shape. A linear baseline correction with a tolerance of 0.2% was employed. The standard errors of the curve-fitting procedure were less than 0.005.

The absorption spectra of the ethanolic solutions of the complexes were acquired in the 700−240 nm range with a UV−visible Spectronic Genexys 2PCC spectrophotometer.

Cyclic voltammetric studies were performed in a three-electrode cell consisting of a platinum working electrode, a platinum counter electrode and a saturated calomel as a reference electrode using a scan rate of 50 mV/s (Solartron potentiostat 1285). The complexes were dissolved in acetonitrile (HPLC grade) containing 0.2 M

(60) Supkowski, R. M.; Horrocks, W. D, Jr. *Inorg. Chim. Acta* **2002**, *340*, 44.

(61) Melby, L. R.; Rose, N. J.; Abramson, E.; Caris, J. C. *J. Am. Chem. Soc.* **1964**, *86*, 5117.

(62) *PeakFit*; Jandel Corporation: San Rafael, CA.

tetrabutylammonium tetrafluoroborate ($TBABF_4$). The electrolyte was purged with nitrogen before each measurement.

A DSC131 Setaram differential scanning calorimeter was used to determine the thermal characteristics of the samples. A disk section (xerogel films) or powder (complexes) with a mass of approximately 20−30 mg was placed in a 40 μL aluminum can and stored in a desiccator over phosphorus pentoxide (P_2O_5) for 1 week at room temperature under a vacuum. After this drying treatment, the cans were hermetically sealed and the thermograms were recorded. Each sample was heated from 25 to 300 °C at 10 °C min^{-1}. The purge gas used in both experiments was high-purity nitrogen supplied at a constant 35 cm^3 min^{-1} flow rate.

Samples for thermogravimetric studies were transferred to open platinum crucibles and analyzed using a Rheometric Scientific TG 1000 thermobalance at a heating rate of 10 °C min^{-1} using dried nitrogen as purging gas (20 mL/min). Prior to measurement, the samples were vacuum-dried at 80 °C for about 48 h and kept in an argon-filled glove box.

The luminescence spectra were recorded at room temperature with a modular double grating excitation spectrofluorimeter with a TRIAX 320 emission monochromator (Fluorolog-3, Jobin Yvon-Spex) coupled to a R928 Hamamatsu photomultiplier, using the front face acquisition mode. The excitation source was a 450 W Xe arc lamp. The emission spectra were corrected for detection and optical spectral response of the spectrofluorimeter and the excitation spectra were corrected for the spectral distribution of the lamp intensity using a photodiode reference detector. The lifetime measurements were acquired with the setup described for the luminescence spectra using a pulsed Xe−Hg lamp (6 μs pulse at half width and 20−30 μs tail). The absolute emission quantum yields were measured at room-temperature using a quantum yield measurement system C9920-02 from Hamamatsu with a 150 W xenon lamp coupled to a monochromator for wavelength discrimination, an integrating sphere as sample chamber, and a multichannel analyzer for signal detection.

The photostability in the UVA spectral region was investigated for 11 h by monitoring the $^5D_0 \rightarrow {}^7F_{0-4}$ integrated emission intensity using a Jobin Yvon-Spex spectrometer (HR 460) coupled to an R928 Hamamatsu photomultiplier, under the continuous excitation of a Xe arc lamp (150 mW) coupled to a Jobin Yvon monochromator (TRIAX 180). The spectra were corrected for the response of the detector.

Conclusions

In this work, we have introduced a novel PCL(530)/siloxane hybrid system doped with two europium complexes (an aquocomplex ($Eu(tta)_3(H_2O)_2$) and a complex lacking labile ligands ($Eu(tta)_3$phen)) with the goal of developing highly luminescent biohybrids with expected applications in environmentally friendly optical devices.

We have fully characterized both complexes from the standpoint of composition, thermal stability, UV−vis features, and IE and EA energies. Whereas doping the PCL(530)/siloxane matrix with the $Eu(tta)_3(H_2O)_2$ complex resulted in a significant enhancement of the $^5D_0$ quantum efficiency (from 29.0% in the complex to 44.2% in the hybrid), the opposite situation occurred when $Eu(tta)_3$phen was added to the same medium, with the $^5D_0$ nonradiative paths in the hybrid being higher than those existing in $Eu(tta)_3$phen itself. Under UVA exposure, the emission intensity of PCL(530)/siloxane/$Eu(tta)_3(H_2O)_2$ decreased 10% in 11 h, whereas that of the PCL(530)/siloxane/$Eu(tta)_3$phen decreased 25%. It is noteworthy that the thermal stability of both doped samples is remarkably high (up to 200 °C).

The data derived from the present investigation lead us to state that a lanthanide aquocomplex containing β-diketonate ligands may be efficiently anchored to the PCL(530)/siloxane host network by means of the carbonyl oxygen atoms of the latter structure, which act as efficient coordinating sites toward the lanthanide ions. In the case of the $Eu(tta)_3(H_2O)_2$ complex, this process resulted in the release of 1 (2) water molecules from the Eu^{3+} coordination shell. When the host matrix was doped with the $Eu(tta)_3$phen complex, the absence of the labile water ligands and the presence of a strongly chelating ligand (i.e., phen) disabled the exchange of coordinating atoms (i.e., the replacement of the water oxygen atoms by the matrix carbonyl oxygen atoms).

The encouraging results reported here reinforce the idea that a simple and attractive way of creating highly luminescent hybrid materials for optics may lie in the choice of the host structure, whose design must provide adequate coordinating groups that play the role of anchoring sites for the guest emitting species. The second requirement that needs to be fulfilled in the light of this concept is the incorporation of the lanthanide species as complexes including simultaneously labile ligands (e.g., water molecules) and β-diketonate ligands. In practical terms, the process of anchoring may be viewed as the formation in situ of a new complex. These issues have been thoroughly discussed very recently by P. P. Lima, et al.[30]

Acknowledgment. This work was supported by Fundação para a Ciência e para a Tecnologia (POCI/CTM/46780/03 and POCI/CTM/40063/01). M.F. acknowledges CQ-VR for a grant.

Supporting Information Available: Figures S1−S4. This material is available free of charge via the Internet at http://pubs.acs.org.

CM062832N